review on the question concludes that this effect is small, if it operates at all.[19] Our intuition in this case calls for interpretation of the effects of the trifluoroacetyl group on spin distribution in terms of electron pair delocalization through the π system, but the reviews cited above appear to leave us with little basis for proposing this. We prefer to postpone further discussion of the problem until the results of our further studies and calculations on these systems become available.

Acknowledgment. We are indebted to Dr. H. Caldararu for recording reference ESR spectra of Fremy salt in water.

(19) Topsom, R. D. *Prog. Phys. Org. Chem.* **1976**, *12*, 1.

Ethylene Biosynthesis. 8. Structural and Theoretical Studies

Michael C. Pirrung

Department of Chemistry, Stanford University, Stanford, California 94305

Received January 20, 1987

The use of semiempirical molecular orbital methods for study of enzymatic reaction mechanisms has been further demonstrated by an investigation of ethylene biosynthesis. Calculations on the neutral forms of amino acids give excellent agreement to experiment. Large variances are found in the energies, however. An X-ray crystal structure of 1-aminocyclopropanecarboxylic acid was carried out to provide a comparison to the calculation. The structural data agree closely with what has previously been found for related molecules. The qualitative findings of the reaction pathway investigation include the following: that the radical SOMO's are carbon-centered; that ring-opening is irreversible; and that the second single-electron oxidation occurs to generate a zwitterion that fragments to ethylene and cyanoformic acid. This hitherto unknown species is calculated to be several kilocalories less stable than its constituents, CO_2 and HCN.

Because of ethylene's importance as a plant ripening hormone, study of its biosynthesis was rejuvenated by the 1979 demonstration that 1-aminocyclopropanecarboxylic acid (ACC, **1**) is its immediate biosynthetic precursor.[1] Research in this area has taken several forms. The feeding of isotopically labeled substrates,[2] the development of chemical models for ethylene production,[3] the evaluation of cell-free systems for ethylene biosynthesis,[4] and the study of substrate analogues have all been used.[5] Currently, the most defensible view of the mechanism of ethylene biosynthesis is that proposed in 1983: namely, the sequential single-electron-transfer mechanism[2a] pictured in Chart I. Some modifications have been made to this scheme to encompass specific oxidants such as are found in the chemical models,[4] and recently a partial kinetic mechanism has been proposed.[2g] While in vivo studies with (sometimes) labeled substrate analogues have given considerable information about the internal workings of the mechanism,[5ac] it seemed necessary to seriously examine the structures and reactivity of some of the intermediates that have previously been postulated. While the enzyme involved in ethylene biosynthesis will clearly have

Table I. Crystal and Data Parameters of 1

A. Crystal Parameters at $T = 25^{a,b}$

empirical formula $C_4H_7NO_2 \cdot {}^1/_2H_2O$

a = 6.2687 (4) Å	space Group $P1$
b = 8.5514 (11) Å	formula weight = 110.2 amu
c = 10.1467 (11) Å	Z = 4
α = 101.763 (10)°	d(calc) = 1.39 g cm^{-3}
β = 96.709 (8)°	μ(calc) = 1.08 cm^{-1}
γ = 94.057 (9)°	
V = 526.3 (2) Å^3	

size: 0.17 × 0.23 × 0.28 mm

B. Data Measurement Parameters[10]

radiation: Mo Kα (λ = 0.71073 Å)
monochromator highly oriented graphite (2θ = 12.2)
detector: crystal scintillation counter, with PHA
reflections measured: $+h, +/-k, +/-l$
2θ range: 3° → 55° scan type: θ–2θ
scan width: $\Delta\theta = 0.65 + 0.35 \tan\theta$
scan speed: 0.78 → 6.7 (θ, deg/min)
background: measured over 0.25(scan width) added to each end of the scan
vert. aperture = 3.0 mm horiz. aperture = 2.3 + 1.0 tan θ mm
no. of unique reflctns collected: 2407
intensity standards (412), (1, −4, −4), (1, −6, 5); measured every hour of X-ray exposure time. Over the data collection period no decrease in intensity was observed.
orientation: Three reflections were checked after every 200 measurements. Crystal orientation was redetermined if any of the reflections were offset by more than 0.1° from their predicted positions. Reorientation was not needed during data collection.

[a] Unit cell parameters and their esd's were derived by at least-squares fit to the setting angles of the unresolved Mo Kα components of 24 reflections with 2θ between 27° and 31°. [b] In this and all subsequent tables the esd's of all parameters are given in parentheses, after the least significant digit(s) of the reported value.

(1) Adams, D. O.; Yang, S. F. *Proc. Natl. Acad. Sci. U.S.A.* **1979**, *76*, 170–174.

(2) (a) Pirrung, M. C. *J. Am. Chem. Soc.* **1983**, *105*, 7207–7209. (b) Pirrung, M. C. *Bioorg. Chem.* **1985**, *13*, 219–226. (c) Adlington, R. M.; Aplin, R. T.; Baldwin, J. E.; Rawlings, B. J.; Osborne, D. *J. Chem. Soc., Chem. Commun.* **1982**, 1086–1087. (d) Adlington, R. M.; Baldwin, J. E.; Rawlings, B. J. *J. Chem. Soc., Chem. Commun.* **1983**, 290–291. (e) Baldwin, J. E.; Adlington, R. M.; Lajoie, G. A.; Rawlings, B. J. *J. Chem. Soc., Chem. Commun.* **1985**, 1496–1498. (f) Peiser, G. D.; Wang, T.-T.; Hoffman, N. E.; Yang, S. F.; Liu, H.-W.; Walsh, C. T. *Proc. Natl. Acad. Sci. U.S.A.* **1984**, *81*, 3059–3063. (g) Pirrung, M. C.; McGeehan, G. M. *J. Am. Chem. Soc.* **1986**, *108*, 5647–5648.

(3) (a) Pirrung, M. C.; McGeehan, G. M. *J. Org. Chem.* **1983**, *48*, 5143–5144. (b) Baldwin, J. E.; Jackson, D. A.; Adlington, R. M.; Rawlings, B. J. *J. Chem. Soc., Chem. Commun.* **1985**, 206–207.

(4) Pirrung, M. C. *Biochemistry* **1986**, *25*, 114–119.

(5) (a) Pirrung, M. C.; McGeehan, G. M. *Angew. Chem., Int. Ed. Engl.* **1985**, *24*, 1044–1045. (b) Pirrung, M. C.; McGeehan, G. M. *J. Org. Chem.* **1986**, *51*, 2103–2106. (c) Baldwin, J. E.; Adlington, R. M.; Rawlings, B. J. *Tetrahedron Lett.* **1985**, *26*, 481–484. (d) Baldwin, J. E.; Adlington, R. M.; Rawlings, B. J.; Jones, R. H. *Tetrahedron Lett.* **1985**, *26*, 485–488. (e) Hoffman, N. E.; Yang, S. F.; Ichihara, A.; Sakamura, S. *Plant Physiol.* **1982**, *70*, 195–199.

0022-3263/87/1952-4179$01.50/0

Chart I. Sequential Single-Electron Transfer Pathway for Ethylene Biosynthesis with Calculated Heats of Formation and SOMO Energies

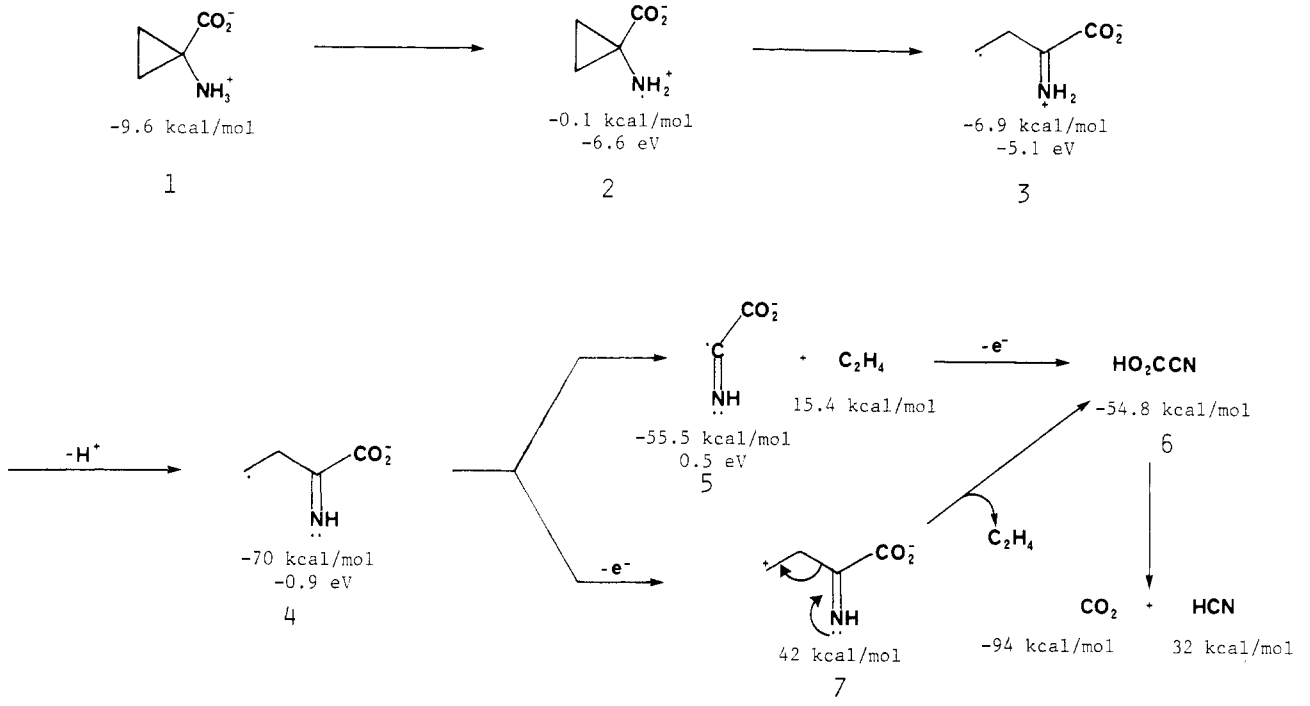

an important influence on the chemistry, information about intrinsic chemical biases may allow the role of the enzyme to be critically examined. Indeed it can be argued that the role of enzymes in promoting chemical transformations has been endowed with unjustified mysticism. As entropy traps and chirotopic environments, enzymes are clearly unequaled, yet they must also obey physical and chemical laws. In the current context, it is difficult to ascribe to the ethylene-forming enzyme any required functions other than substrate recognition and electron removal, as will be exposed below.

Because computational study has proven useful for enzymes bearing some similarities to that producing ethylene,[6] a semiempirical MO study of the proposed mechanism for ethylene biosynthesis has been undertaken. In order to compare some of the results to experiment, an X-ray crystal structure determination on ACC has been completed. A more reasonable mechanistic picture has been developed, and the utility of the computational method for examining amino acids has been demonstrated.

Methods

Theory. MNDO[7] calculations were performed with Owens' modification of the QCPE version[8] on an IBM PC-XT with Fast-88 accelerator board. The program was checked by comparison with Schleyer's results on cyclopropylamine.[9]

Structure of ACC. Colorless, lumpy crystals were obtained by slow crystallization from a hot-filtered, saturated solution (3:1 EtOH/H_2O). Some of these crystals were mounted on glass fiber by using polycyanoacrylate cement. Preliminary photographs indicated no particular Laue symmetry. The crystal used for data collection was then transferred to an Enraf-Nonius CAD-4 diffractometer[10] and centered in the beam. Automatic peak search and indexing procedures yielded a triclinic reduced primitive cell.

Table II. Positional Parameters and Their Estimated Standard Deviations[a]

atom	x	y	z	B(A2)	occ.
O1	−0.1178 (2)	0.2990 (1)	0.3102 (1)	3.12 (2)	
O2	0.0039 (3)	0.2038 (2)	0.1138 (2)	3.86 (4)	0.60
O2′	−0.0790 (5)	0.2653 (4)	0.0900 (3)	4.07 (6)*	0.40
O3	−0.2110 (2)	−0.3347 (1)	0.4155 (1)	2.83 (2)	
O4	−0.4961 (2)	−0.1970 (1)	0.4442 (1)	2.42 (2)	
O5	−0.3266 (3)	0.0259 (2)	−0.0769 (2)	3.05 (3)	0.65
O5′	−0.3679 (6)	0.0952 (4)	−0.0662 (4)	3.81 (6)*	0.35
N1	0.1977 (2)	0.5342 (1)	0.3947 (1)	2.10 (2)	
N2	−0.3663 (2)	0.0279 (1)	0.3122 (1)	1.94 (2)	
C1	−0.0042 (3)	0.3112 (2)	0.2200 (2)	3.34 (3)	
C2	0.1850 (2)	0.4379 (2)	0.2558 (1)	2.24 (2)	
C3	0.3934 (3)	0.4029 (2)	0.2025 (2)	3.57 (3)	
C4	0.2601 (3)	0.5201 (2)	0.1500 (2)	3.23 (3)	
C5	−0.3187 (2)	−0.2210 (1)	0.4009 (1)	1.82 (2)	
C6	−0.2324 (2)	−0.1046 (1)	0.3229 (1)	1.87 (2)	
C7	0.0075 (2)	−0.0714 (2)	0.3294 (2)	3.32 (3)	
C8	−0.1224 (3)	−0.1690 (2)	0.2024 (2)	3.59 (3)	
H1A	0.311 (3)	0.619 (2)	0.418 (2)	1.1 (3)*	
H1B	0.065 (3)	0.592 (2)	0.409 (2)	1.4 (4)*	
H1C	0.223 (3)	0.468 (2)	0.462 (2)	1.6 (4)*	
H2A	−0.421 (3)	0.065 (2)	0.399 (2)	1.5 (4)*	
H2B	−0.480 (3)	0.001 (2)	0.242 (2)	0.8 (3)*	
H2C	−0.284 (3)	0.121 (2)	0.295 (2)	1.8 (4)*	
H3A	0.526 (3)	0.455 (2)	0.269 (2)	2.5 (4)*	
H3B	0.402 (3)	0.299 (3)	0.148 (2)	2.6 (5)*	
H4A	0.316 (3)	0.638 (2)	0.185 (2)	2.1 (4)*	
H4B	0.180 (3)	0.488 (2)	0.061 (2)	1.8 (4)*	
H7A	0.060 (3)	0.038 (2)	0.332 (2)	1.1 (3)*	
H7B	0.089 (3)	−0.126 (2)	0.381 (2)	2.0 (4)*	
H8A	−0.144 (3)	−0.115 (2)	0.127 (2)	1.8 (4)*	
H8B	−0.113 (3)	−0.289 (2)	0.181 (2)	1.7 (4)*	
H5A	−0.240 (4)	0.114 (3)	−0.012 (3)	5.1 (6)*	
H5B	−0.4570	0.0292	−0.0273	4.0*	0.50
H5C	−0.2070	−0.0273	−0.0820	4.0*	0.50

[a] Starred atoms were included with isotropic thermal parameters. The thermal parameter given for anisotropically refined atoms is the isotropic equivalent thermal parameter defined as $^4/_3[a^2B(1,1) + b^2B(2,2) + c^2B(3,3) + ab(\cos\gamma)B(1,2) + ac(\cos\beta)B(1,3) + bc(\cos\alpha)B(2,3)]$, where a, b, and c are real cell parameters and $B(i,j)$ are anisotropic β's.

(6) Merkelbach, I. I.; Becht, H. G. M.; Buck, H. M. *J. Am. Chem. Soc.* **1985**, *107*, 4037–4042. Shea, J. P.; Nelson, S. D.; Ford, G. P. *J. Am. Chem. Soc.* **1983**, *105*, 5451–5454. Salem, L.; Eisenstein, O.; Anh, N. T.; Burg, H. B.; Devaquet, A.; Segal, G.; Veillard, A. *Nouv. J. Chim.* **1977**, *1*, 335.
(7) Dewar, M. J. S.; Theil, W. J. *J. Am. Chem. Soc.* **1977**, *99*, 4899–4907, 4907–4917.
(8) Thiel, W. *QCPE* **1979**, No. 379.
(9) Clark, T.; Spitznagel, G. W.; Klose, R.; Schleyer, P. v. R. *J. Am. Chem. Soc.* **1984**, *106*, 4412–4419.

Table III. Intramolecular Distances (Å)

atom 1	atom 2	distance	atom 1	atom 2	distance
C1	O1	1.239 (1)	C5	O3	1.245 (1)
C1	O2	1.274 (2)	C5	O4	1.257 (1)
C1	O2′	1.317 (2)	C5	C6	1.501 (1)
C1	C2	1.506 (1)	C6	N2	1.471 (1)
C2	N1	1.470 (1)	C6	C7	1.502 (1)
C2	C3	1.498 (1)	C6	C8	1.501 (1)
C2	C4	1.500 (1)	C7	C8	1.497 (2)
C3	C4	1.489 (2)	N2	H2A	0.980 (12)
N1	H1A	0.952 (12)	N2	H2B	0.925 (12)
N1	H1B	1.004 (12)	N2	H2C	0.971 (13)
N1	H1C	0.981 (13)	C7	H7A	0.961 (12)
C3	H3A	1.020 (14)	C7	H7B	0.911 (13)
C3	H3B	0.950 (15)	C8	H8A	0.976 (13)
C4	H4A	1.023 (13)	C8	H8B	1.014 (12)
C4	H4B	0.956 (13)			

Inspection of the Niggli values[11] revealed no conventional cell of higher symmetry. The final cell parameters and specific data collection parameters for this data set are given in Table I.

The 2407 unique raw intensity data were converted to structure factor amplitudes and their esd's by correction for scan speed, background, and Lorentz and polarization effects.[12-14] No correction for crystal decomposition or absorption was necessary. The choice of the centric space group was confirmed by the successful solution and refinement of the structure.

The structure was solved by direct methods (MULTAN) and refined via standard least-squares and Fourier techniques. Hydrogen atoms were included in the least-squares refinement, except for the two disordered hydrogens attached to the water molecule, which were included in their positions as determined from a difference map, but not refined. The disorder in the positions of the water molecule and of the one oxygen atom in the amino acid was modeled by modifying the occupancy and checking the residuals and equivalent thermal parameters. Toward the end of refinement two reflections, the (0, 0, −1) and the (0, −1, 0), were removed from the refinement due to measurement errors.

The final residuals[15] for 204 variables refined against the 1997 data for which $F^2 > 3\sigma(F^2)$ were $R = 3.88\%$, $wR = 5.91\%$, and GOF = 2.84. The R value for all 2407 data was 6.14%. The high value for the GOF residual is likely due to small errors in the modeling of the disorder, especially with respect to hydrogen bonding and possible low-occupancy sites for the water oxygen.

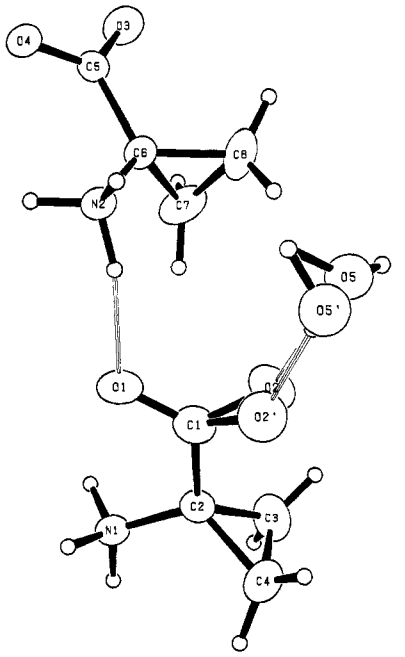

Figure 1. Diagram showing both molecules of the acid and the water molecule. The minority components of the disorder are labeled with a ′. Hydrogen atoms are unlabeled for clarity but are numbered according to their attached atoms. The ellipsoids are scaled to represent the 50% probability surface. Hydrogens are given as arbitrarily small spheres for clarity.

The quantity minimized by the least-squares program was $\sum w(|F_o| - |F_c|)^2$, where w is the weight of a given observation. The p-factor,[15] used to reduce the weight of intense reflections, was set to 0.03 throughout the refinement. The analytical forms of the scattering factor tables for the neutral atoms were used[16] and all scattering factors were corrected for both the real and imaginary components of anomalous dispersion.[17]

Inspection of the residuals ordered in ranges of $\sin(\theta)/\lambda$, $|F_o|$, and parity and value of the individual indexes showed no unusual features or trends. The largest peak in the final difference Fourier map had an electron density of 0.23 $e^-/Å^3$, and the lowest excursion −29 $e^-/Å^3$. There was no indication of significant sec-

(10) Instrumentation at the University of California Chemistry Department X-ray Crystallographic Facility (CHEXRAY) consists of two Enraf-Nonius CAD-4 diffractometers using software described in the CAD-4 Operation Manual, Enraf-Nonius, Delft, Nov 1977, updated Jan 1980.

(11) Roof, R. B., Jr. *A Theoretical Extension of the Reduced-Cell Concept in Crystallography*, Publication LA-4038; Los Alamos Scientific Laboratory, Los Alamos: New Mexico, 1969.

(12) Calculations were performed on DEC Microvax II using locally modified Nonius-SDP[3] software operating under Micro-VMS operating system.

(13) Structure Determination Package User's Guide, 1985, B. A. Frenz and Associates, Inc., College Station, TX 77840.

(14) The data reduction formulae are

$$F_o^2 = \frac{\omega}{\mathrm{Lp}}(C - 2B)$$

$$\sigma_o(F_o^2) = \frac{\omega}{\mathrm{Lp}}(C + 4B)^{1/2}$$

$$F_o = (F_o^2)^{1/2}$$

$$\sigma_o(F) = (F_o^2 + \sigma_o(F_o^2))^{1/2} - F_o$$

where C is the total count in the scan, B the sum of the two background counts, ω is the scan speed used in deg/min, and

$$\frac{1}{\mathrm{Lp}} = \frac{\sin 2\theta\,(1 + \cos^2 2\theta_m)}{1 + \cos^2 2\theta_m - \sin^2 2\theta}$$

is the correction for Lorentz and polarization effects for a reflection with scattering angle 2J and radiation monochromatized with a 50% perfect single-crystal monochrometer with scattering angle $2\theta_m$.

(15)

$$R = \frac{\sum||F_o| - |F_c||}{\sum|F_o|}$$

$$wR = \left\{\frac{\sum w(|F_o| - |F_c|)^2}{\sum wF_o^2}\right\}^{1/2}$$

$$\mathrm{GOF} = \left\{\frac{\sum w(|F_o| - |F_c|)^2}{(n_o - n_v)}\right\}^{1/2}$$

where n_o is the number of observations, n_v the number of variable parameters, and the weights w were given by

$$w = \frac{1}{\sigma^2(F_o)}$$

$$\sigma(F_o^2) = (\sigma_o^2(F_o^2) + (pF^2)^2)^{1/2}$$

where $\sigma^2(F_o)$ is calculated as above from $\sigma(F_o^2)$ and where p is the factor used to lower the weight of intense reflections.

(16) Cromer, D. T.; Waber, J. T. *International Tables for X-ray Crystallography*, Vol. IV; The Kynoch Press: Birmingham, England, 1974; Table 2.2B.

(17) Cromer, D. T., ref 16, Table 2.3.1.

Table IV. Intramolecular Angles (deg)

atom 1	atom 2	atom 3	angle
C2	C1	O1	117.17 (8)
C2	C1	O2	114.62 (10)
C2	C1	O2′	115.98 (13)
O1	C1	O2	125.59 (10)
O1	C1	O2′	122.26 (13)
N1	C2	C1	112.65 (7)
N1	C2	C3	117.38 (8)
N1	C2	C4	117.45 (7)
C1	C2	C3	119.63 (8)
C1	C2	C4	120.58 (8)
C3	C2	C4	59.57 (7)
C2	C3	C4	60.26 (6)
C3	C4	C2	60.17 (7)
C2	N1	H1A	114.3 (7)
C2	N1	H1B	112.2 (7)
C2	N1	H1C	111.1 (7)
H1A	N1	H1B	102.7 (9)
H1A	N1	H1C	105.9 (9)
H1B	N1	H1C	110.1 (9)
C2	C3	H3A	113.1 (7)
C2	C3	H3B	118.1 (8)
C4	C3	H3A	113.8 (8)
C4	C3	H3B	121.1 (8)
H3A	C3	H3B	117.7 (11)
C2	C4	H4A	114.7 (7)
C2	C4	H4B	116.1 (8)
C3	C4	H4A	115.8 (7)
C3	H4	H4B	118.6 (7)
H4A	C4	H4B	118.3 (11)
H5A	O5	H5B	95.7
H5A	O5	H5C	88.5
H5B	O5	H5C	138.4
H5A	O5′	H5B	105.9
C6	C5	O3	117.46 (7)
C6	C5	O4	117.17 (7)
O3	C5	O4	125.36 (7)
N2	C6	C5	114.31 (6)
N2	C6	C7	117.91 (7)
N2	C6	C8	116.90 (7)
C5	C6	C7	119.06 (7)
C5	C6	C8	118.26 (7)
C7	C6	C8	59.82 (8)
C6	C7	C8	60.04 (6)
C7	C8	C6	60.14 (6)
C6	N2	H2A	109.7 (7)
C6	N2	H2B	113.1 (6)
C6	N2	H2C	112.0 (7)
H2A	N2	H2B	109.7 (9)
H2A	N2	H2C	105.9 (10)
H2B	N2	H2C	106.1 (10)
C6	C7	H7A	116.0 (7)
C6	C7	H7B	115.5 (8)
C8	C7	H7A	119.2 (7)
C8	C7	H7B	116.3 (8)
H7A	C7	H7B	117.2 (11)
C6	C8	H8A	115.7 (7)
C6	C8	H8B	116.3 (7)
C7	C8	H8A	115.6 (7)
C7	C8	H8B	118.2 (7)
H8A	C8	H8B	118.0 (10)
N1	H1A	O4	170.6 (10)
N1	H1B	O3	169.6 (10)
N1	H1C	O3	168.5 (10)
N2	H2A	O4	163.0 (10)
N2	H2B	O5	166.3 (10)
N2	H2B	O5′	158.5 (10)
N2	H2C	O1	165.3 (11)
O5	H5A	O2	153.5 (16)
O5	H5A	O2′	175.4 (16)
O5	H5B	O5	161.9
O5	H5B	O5′	142.4
O5	H5B	O5′	158.0
O5	H5C	O2	163.1

ondary extinction in the high-intensity low-angle data.

The positional and thermal parameters of the atoms are given in the tables. Anisotropic thermal parameters as well as a listing of the values of F_o and F_c are available as supplementary material. Distances and angles are also given in the tables. Internal comparison of the two independent molecules (see Figure 1) shows that they are in excellent agreement with each other except in the immediate region of the disorder of O2, as might be expected. The disorder of O2 can be understood if one looks at the packing diagram (Figure A, supplementary material). A hydrogen bond can be donated by O5 to either one of the two possible O2 positions, or to both, depending on whether that particular O5 is donating or receiving the hydrogen bond to the next water molecule (related by the center of inversion in the average structure reported by the X-ray experiment).

The structure has two independent molecules in dissimilar environments, so there is no possibility that there is a higher symmetry space group involved. There are eight hydrogens (net) in the structure, and they each participate in a hydrogen bond.

Table V. Comparison of Calculated and Experimental Data for Glycine

parameter	zwitter-ion (expt)	neutral (calc)	zwitter-ion (calc)	radical cation (calc)
		Bond Lengths (Å)		
C1O1	1.25	1.23	1.25	1.22
C1O2	1.25	1.36	1.25	1.33
C2N	1.48	1.46	1.52	1.41
C1C2	1.53	1.54	1.62	1.61
NH1	1.05	1.01	1.02	1.01
NH2	1.04	1.01	1.02	1.01
NH3	1.03		1.02	
C2H4	1.09	1.12	1.11	1.12
C2H5	1.09	1.12	1.11	1.12
		Bond Angles (deg)		
C2C1O1	117.4	115.1	114.8	
C2C1O2	117.1		114.6	
O1C1O2	125.5	126.1	130.6	
C1C2N	111.8	115.0	107.4	
C2NH1	112.1	111.3	110.9	
C2NH2	112.0		112.4	
C2NH3	110.3	111.1	110.0	
C1C2H4	108.7	108.1	112.4	
C1C2H5	110.4	109.8	112.2	

Results

An initial measure of the utility of semiempirical methods applied to amino acids was obtained by studying glycine. As Table V shows for representative parameters, reasonable agreement with known[18] structural data is obtained. In the zwitterion, large deviations for the C–CO_2 and C–N bond lengths are found. The much better agreement in the neutral form suggests that it is the most representative species for computational study. While the prevalence of the zwitterionic form is well-known in solution, the neutral is favored in the gas phase.[19] The heat of formation of −95 kcal/mol calculated for the neutral differs far less from experiment (−128.5 kcal/mol) than does that for the zwitterion. Clearly, it will be difficult to obtain absolute energies for the intermediates in the pathway by using this method, but qualitative trends as well as comparisons between isomers should be possible.

The glycine radical cation was also studied for comparison to ACC (vide infra). Previously, Bauld and coworkers have validated MNDO as a tool to examine cation radicals and argued[20] that the C–C bond lengthening in glycine radical cation is evidence for a weak, one-electron bond. Not mentioned by Bauld is the commensurate shortening of the C–N bond and the appreciable spin

(18) Narayanan, P.; Venkataraman, S. *J. Cryst. Mol. Struct.* **1975**, *5*, 15–26. Power, L. F.; Turner, K. E.; Moore, F. H. *Acta Crystallogr., Sect. B* **1976**, *B32*, 11–16.

(19) Locke, M. J.; McIver, R. *J. Am. Chem. Soc.* **1983**, *105*, 4226–4232.

(20) Bellville, D.; Pabon, R.; Bauld, N. *J. Am. Chem. Soc.* **1985**, *107*, 4979–4980.

Chart II. Heats of Formation (kcal/mol) of Selected Isomers of 3. All Are Geometry-Optimized Local Minima

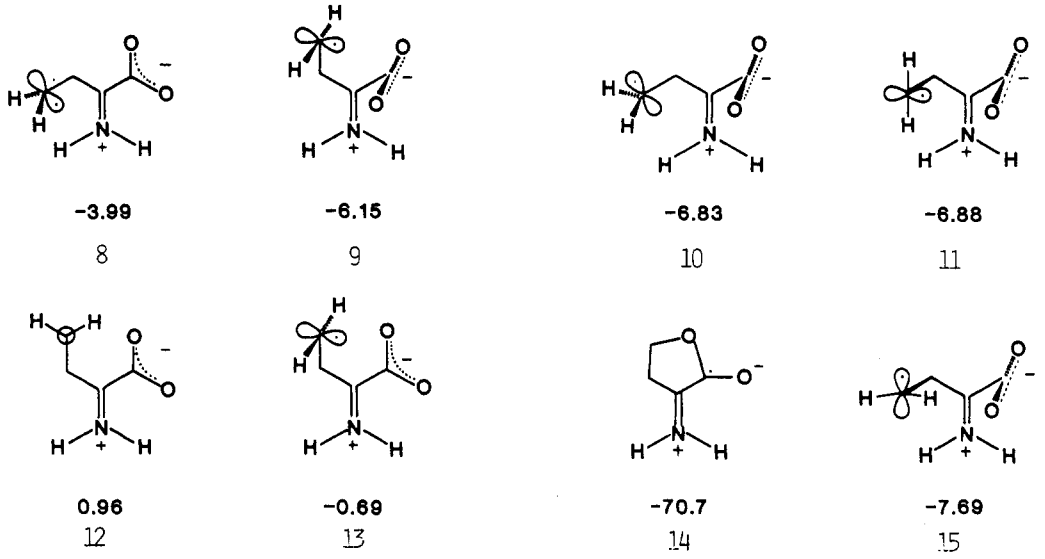

density on the planarized nitrogen. This species may be viewed as an intermediate in a path toward aminomethyl radical and CO_2.

In order to have a structural basis for calculation on ACC, not to mention the importance such a structure would have in active site mapping and analogue design, an X-ray diffraction analysis was undertaken. Two previous studies of ACC relatives (a metal complex[21] and an alkylated analogue[5d]) have been conducted. The present results are summarized in the Experimental Section, supplementary material, and ORTEP plot in Figure 1. Noteworthy features include the disorder of the carboxylate oxygen of one molecule in the unit cell and the favored C2–N1 rotamer. Excellent agreement is found to previous work.

Two C_s conformers (perpendicular and bisected, NH_3 as in Figure 1) of ACC (zwitterion) were studied by using MNDO. Their heats of formation are quite similar, suggesting a small C–CO_2 rotational barrier and minimal cyclopropane–carboxyl conjugation. They also have only trivial structural differences. Their structural parameters deviate most from experiment (Table VI) in the cyclopropane. This deviation likely stems from the known problems MNDO has with small rings. As in the case of glycine, the situation improves in the neutral form where the 0.05 Å discrepancy in the C2–C3 distance is comparable to the 0.04 Å error in the calculated cyclopropylamine structure.[22] Other species formed by proton and/or electron removal are included in the table for comparison. These are potential intermediates in the production of **2**, though these studies can say nothing about which path to **2** is used in vivo.

The ACC anion is also of interest because that form is oxidized electrochemically in a model for ethylene production.[2a] Structural agreement of the calculation with

Table VI. Comparison of Calculated Bond Lengths (Å) for Forms of ACC

	zwitterion (1)	neutral	anion	radical zwitterion (2)
C1–O1	1.241	1.231	1.260	1.237
C1–O2	1.248	1.357	1.259	1.236
C1–C2	1.617	1.523	1.567	1.682
C2–N	1.495	1.451	1.460	1.402
C2–C3	1.537	1.552	1.543	1.539
C2–C4	1.537	1.552	1.544	1.539
C3–C4	1.523	1.514	1.521	1.527
ΔH_f(kcal/mol)				
perpendicular	−9.66	−70.83	−86.47	2.87
bisected	−9.56	−71.69	−87.55	−0.06

experiment is adequate. The two carboxyl rotamers are again of comparable stability. That the heat of formation is calculated to be much more negative than that of **1** is contrary to experimental data for glycine in the gas phase.[19] The ionization potential of 4.2 eV compares to 10.3 eV calculated for cyclopropylamine. While the HOMO's of both are quite delocalized, the former is primarily carboxyl-like, with some nitrogen contribution. The difference in HOMO energies qualitatively accounts for the easier electrochemical oxidation of ACC (anion) compared to cyclopropylamine or cyclopropanecarboxylate.[2a] Further information on this point was obtained from study of the radical zwitterion **2**, a crucial intermediate in the postulated mechanism. Structurally, the two C_s conformers are again quite similar, with the bisected form qualitatively more stable. Spin is heavily delocalized to N, O, and C atoms, corroborating the above conclusions on ease of oxidation. The changes observed compared to the neutral form are similar to the glycine case, namely, lengthening of the C1–C2 bond and shortening the C–N bond. A more acute cyclopropane–carboxyl bond angle is also evident, but nitrogen planarization is absent. These changes signal an intermediate in a decarboxylation reaction; surprisingly, no evidence for the expected ring-opening reaction was found in C–C bond lengths.

Intermediate **3** in Chart I is also crucial in the postulated mechanism for ethylene production. Its presence has been inferred from studies using isotopic labeling[2a] and free radical clocks.[5a] Since it no longer bears the constraints of the cyclopropane ring, its conformational possibilities are great. While a complete exploration of this conformational energy surface has not been conducted, the results partially summarized in Chart II (includes heats of

(21) Wanjek, H.; Nagel, U.; Beck, W. *Chem. Ber.* **1985**, *118*, 3258–3267.
(22) Rall, M.; Harmony, M. D.; Cassada, D. A.; Staley, S. W. *J. Am. Chem. Soc.* **1986**, *108*, 6184–6189.

formation of geometry-optimized local minima; **8**, **9**, **12–14** C_s) suggest it is relatively flat. While **15** is of lowest energy, three other structures are also worth considering. The first is **11**, which is expected to be produced immediately upon ring opening. The second is **14**, which skeptics of the mechanism suggest would be more stable than any form of **3**. It should be noted, though, that **14** is better represented as a neutral enol radical, and gas-phase calculations may exaggerate the instability of zwitterions **8–13** relative to **14**. Another conformer, **13**, represents **3** as it is prepared to cyclize. Its energy suggests a barrier to cyclization that may permit other processes to dominate (vide infra).

Other interesting features of intermediate **3** include a localized carbon radical as the SOMO and a preferred orthogonal relationship of the carboxylate and Schiff's base. The 7 kcal/mol exothermicity calculated for the **2** → **3** conversion compares to a value of 3.2 kcal/mol measured for cyclopropyl carbinyl.[23] This value is also consistent with conclusions from isotope-effect studies that the ring-opening step has a large forward commitment.[2g]

While intermediates **1–3** stand on firm experimental ground, the continued exploration of the mechanism is more speculative. Because another single-electron oxidation must be performed and no readily oxidized sites are apparent, a deprotonation of **3** was proposed.[2a] This produces **4**, which again has myriad conformational possibilities. Geometry optimizations from over 20 starting points indicate little pronounced preference. All have carbon-centered SOMO's, and therefore may represent species like those that were observed in a spin-trapping study of ACC oxidation.[24] The only significant structural change is shortening of the C–CO_2 bond, which is likely a peculiarity of MNDO as applied to amino acids (vide supra). Information concerning these species is provided in the supplementary material.

Two reaction paths have been considered for **4**. A second one-electron oxidation was postulated to occur at nitrogen,[2a] but the results above suggest that oxidation to the carbonium ion is more likely. Geometry optimization was therefore conducted on selected conformers of **7**. These fall into three classes: the most stable are those that can (and do) close to the lactone (ΔH_f ca. −28 kcal/mol); the least stable possess no hyperconjugation; those of intermediate stability hyperconjugate the empty p orbital with the C2–C3 bond. The most dramatic structural changes accompany hyperconjugation, including a 0.05-Å shortening of the C3–C4 bond, a 0.08-Å lengthening of the C2–C3 bond, a 0.03-Å shortening of the C2–N bond. Clearly this represents a species that is tending toward ethylene loss. A Grob fragmentation to give ethylene and cyanoformic acid would be highly exothermic. Alternatively, it was postulated[4] that **4** might yield ethylene and cyanoformate-radical anion (**5**) directly. An almost linear geometry and highly delocalized spin are calculated for **5**, but its production from **4** is thermodynamically uphill. Furthermore, the lack of significant structural changes signaling imminent ethylene loss mitigates against the *spontaneous* **4** → **5** conversion. Conversely, production of **7** could be *driven* by a powerful (enzymatic) oxidant. One problem with the enzymatic oxidation of **4** is that the oxidant must move over 3 Å from the site of initial oxidation, but it has the virtue that in this step all of the thermodynamic price is paid.

Whether obtained by oxidation of **5**, fragmentation of **7**, or by other means,[3a] cyanoformic acid has proved a crucial element in many schemes for ethylene production. While citations to this compound exist, they are erroneous; it has never been observed. It is an attractive intermediate in ethylene biosynthesis as a source of hydrogen cyanide and CO_2. A calculated heat of formation of −55 kcal/mol suggests a greater than 5 kcal/mol exothermicity for its conversion to these constituents.

A fascinating element of ethylene biosynthesis concerns alkylated ACC analogues. Despite the fact that the natural substrate is achiral, the ethylene-synthesizing system discriminates between stereoisomers of methyl- and ethyl-ACC.[5be] Indeed, this capability is the sine qua non of validity for cell-free systems. Because some purely chemical oxidants show smaller, though real, levels of stereodiscrimination as well,[4] alkyl-ACC's were studied. Full geometry optimization on radical zwitterions derived from (1*R**,2*S**)- and (1*R**,2*R**)-methyl-ACC suggest that the former is nominally (~1 kcal/mol) more stable. Applying the Hammond postulate and the knowledge that production of the radical cation is rate limiting,[2g] the 1*R**,2*S** derivative is predicted to react faster, as is observed.

Summary

This study has shown that semiempirical molecular orbital calculations can be used to predict structures of unobservable reactive intermediates in enzymatic reactions. Qualitative energy information may also be obtained. As concerns ethylene production, the method has provided explanations for varying redox potentials and stereoselectivity. It has suggested that a hitherto unconsidered intermediate, zwitterion **7**, possesses appropriate characteristics for an ethylene precursor both in the electrochemical model and in vivo.

Acknowledgment. Calculations were (in part) supported by Grant Number CHE-8312693 from the National Science Foundation. M.C.P. is a Presidential Young Investigator (NSF CHE 84-51324) and a Research Fellow of the Alfred P. Sloan Foundation. The assistance of Dr. Fred Hollander of the University of California CHEXRAY facility concerning the X-ray crystal structure is gratefully acknowledged.

Note Added in Proof: A more detailed study of the mechanism of the model reaction discussed in ref 4 has appeared: Gardner, H. W.; Newton, J. W. *Phytochemistry* **1987**, *26*, 621–626.

Supplementary Material Available: Table of anisotropic thermal parameters, packing diagram, and summaries of structural data for **4** and **7** (3 pages); observed and calculated structure factors for **1** (14 pages). Ordering information is given on any current masthead page.

(23) Effio, A.; Griller, D.; Ingold, K. U.; Beckwith, A. L. J.; Serelis, A. K. *J. Am. Chem. Soc.* **1980**, *102*, 1734–1736.

(24) Legge, R.; Thompson, J. *Plant Cell Physiol.* **1982**, *23*, 171. McRae, D.; Coker, J.; Legge, R.; Thompson, J. *Plant Physiol.* **1983**, *73*, 784.